T-helper-1-cell cytokines drive cancer into senescence

Braumüller, Heidi ; Wieder, Thomas ; Brenner, Ellen ; Aßmann, Sonja ; Hahn, Matthias ; Alkhaled, Mohammed ; Schilbach, Karin ; Essmann, Frank ; Kneilling, Manfred ; Griessinger, Christoph ; Ranta, Felicia ; Ullrich, Susanne ; Mocikat, Ralph ; Braungart, Kilian ; Mehra, Tarun ; Fehrenbacher, Birgit ; Berdel, Julia ; Niessner, Heike ; Meier, Friedegund ; van den Broek, Maries ; Häring, Hans-Ulrich ; Handgretinger, Rupert ; Quintanilla-Martinez, Leticia ; Fend, Falko ; Pesic, Marina ; Bauer, Jürgen ; Zender, Lars ; Schaller, Martin ; Schulze-Osthoff, Klaus ; Röcken, Martin

Abstract: Cancer control by adaptive immunity involves a number of defined death and clearance mechanisms. However, efficient inhibition of exponential cancer growth by T cells and interferon- (IFN-) requires additional undefined mechanisms that arrest cancer cell proliferation. Here we show that the combined action of the T-helper-1-cell cytokines IFN- and tumour necrosis factor (TNF) directly induces permanent growth arrest in cancers. To safely separate senescence induced by tumour immunity from oncogene-induced senescence, we used a mouse model in which the Simian virus 40 large T antigen (Tag) expressed under the control of the rat insulin promoter creates tumours by attenuating p53- and Rb-mediated cell cycle control. When combined, IFN- and TNF drive Tag-expressing cancers into senescence by inducing permanent growth arrest in G1/G0, activation of p16INK4a (also known as CDKN2A), and downstream Rb hypophosphorylation at serine 795. This cytokine-induced senescence strictly requires STAT1 and TNFR1 (also known as TNFRSF1A) signalling in addition to p16INK4a. In vivo, Tag-specific T-helper 1 cells permanently arrest Tag-expressing cancers by inducing IFN- - and TNFR1-dependent senescence. Conversely, Tnfr1(-/-)Tag-expressing cancers resist cytokine-induced senescence and grow aggressively, even in TNFR1-expressing hosts. Finally, as IFN- and TNF induce senescence in numerous murine and human cancers, this may be a general mechanism for arresting cancer progression.

DOI: https://doi.org/10.1038/nature11824

T_H1 Cell Cytokines Drive Cancer into Senescence

Heidi Braumüller[1,#], Thomas Wieder[1#], Sonja Fischer[1], Ellen Brenner[1], Matthias Hahn[1], Mohammed Alkhaled[2], Karin Schilbach[2], Frank Essmann[3], Manfred Kneilling[1], Christoph Griessinger[1,4], Felicia Ranta[5], Susanne Ullrich[5], Ralph Mocikat[6], Kilian Braungart[1], Tarun Mehra[1], Birgit Fehrenbacher[1], Maries van den Broek[7], Hans-Ulrich Häring[5], Rupert Handgretinger[2], Leticia Quintanilla-Martinez[8], Falko Fend[8], Martin Schaller[1], Klaus Schulze-Osthoff[3], Martin Röcken[1]*

[#]HB and TW contributed equally

*Correspondence: mrocken@med.uni-tuebingen.de

[1]Dept. of Dermatology, Eberhard Karls University, Liebermeisterstr. 25, 72076 Tübingen, Germany

[2]Dept. of General Pediatrics, Oncology/Hematology, Eberhard Karls University, Hoppe-Seyler-Str. 1, 72076 Tübingen, Germany

[3]Interfaculty Institute for Biochemistry, Eberhard Karls University, Hoppe-Seyler-Str. 4, 72076 Tübingen, Germany

[4]Laboratory for Preclinical Imaging and Imaging Technology of the Werner Siemens-Foundation, Department for Preclinical Imaging and Radiopharmacy, Eberhard Karls University, Röntgenweg 13, 72076 Tübingen, Germany

[5]Dept. of Internal Medicine IV, Endocrinology, Diabetology and Clinical Chemistry, Eberhard Karls University, Otfried-Müller-Str. 10, 72076 Tübingen, Germany

[6]Institute for Molecular Immunology, Helmholtz Center Munich, Marchioninistr. 25, 81377 München, Germany

[7]Clinic of Oncology, University Hospital Zurich, Raemistrasse 100, 8091 Zurich, Switzerland

[8]Dept. of Pathology, Eberhard Karls University, Liebermeisterstr. 8, 72076 Tübingen, Germany

SUMMARY

Cancer control by adaptive immunity involves numerous death[1-8] and clearance[9-11] mechanisms. Yet, efficient inhibition of exponential cancer growth by T-cells and interferon-γ (IFN-γ) strictly requires additional, so far undefined mechanisms that arrest cancer cell proliferation[1-5,12,13]. Here we show that the combined action of the T-helper 1 (T_H1)-cell cytokines IFN-γ and tumor-necrosis-factor (TNF) directly induces permanent growth arrest in cancers. To safely separate senescence induced by tumor-immunity from oncogene-induced senescence[9-11,14-17], we used RIP1-Tag2 mice, where large T-antigen (Tag) causes cancer by attenuating p53- and Rb-mediated cell cycle control[18,19]. When combined, IFN-γ and TNF drive Tag-expressing cancers into senescence, as they induce permanent growth arrest in G_1/G_0, activation of $p16^{Ink4a}$, downstream Rb-hypophosphorylation at Ser795, and E2F2 suppression. This cytokine-induced senescence strictly requires STAT1- and TNFR1-signaling. Also *in vivo,* Tag-specific T_H1-cells permanently arrest Tag-expressing cancers by inducing IFN-γ- and TNFR1-dependent senescence. Therefore, $TNFR1^{-/-}$xRIP1-Tag2 cancers resist to cytokine-induced senescence and grow aggressively, even in TNFR1-expressing hosts. Moreover, IFN-γ and TNF induce senescence in murine breast cancers and human rhabdomyosarcoma, revealing IFN-γ/TNF - induced senescence as a general mechanism arresting cancer progression.

Recent studies from targeted cancer immunotherapies show that adaptive immunity can efficiently control human cancer[20-24]. Surprisingly, many cancer immunotherapies do not cause cytotoxic cancer elimination but arrest cancer growth or induce slow cancer regression[21,22], even though immunotherapies generally focus on $CD8^+$ cytotoxic T lymphocytes (CTL) or natural killer cells[1-8,23,24]. Moreover, where studied, growth arrest and cancer regression correlate with tumor-specific, IFN-γ producing $CD4^+$ (T_H1) cells rather than CTL[20-23]. In addition, profiling of patients in clinical cancer trials shows a critical role for IFN-γ and TNF in cancer control[25,26].

Similarly, efficient immune control of murine cancers resulting from aberrant cell cycle control, oncogene expression, chemical or viral transformation strictly requires IFN-γ[3-7,12,27]. In consequence, IFN-γ- and TNF-producing T_H1 cells specific for the tumor antigen Tag (Tag-T_H1) restrain Tag-induced islet cancers in mice expressing Tag under the control of the rat insulin promotor1 (RIP1-Tag2) in all pancreatic islet cells[12,18]. T_H1-immunity doubles life span of mice through strictly IFN-γ- and TNFR1-dependent mechanisms[12], without causing detectable signs of cytotoxicity, tumor cell necrosis, or apoptosis[12]**.** This is surprising, as Tag-expression causes invasive β-cell cancers (β-cancer) in 2% of the islets by incomplete retinoblastoma (Rb) suppression and p53 silencing[18,19].

Only $CD4^+$ T_H1 cells that produce IFN-γ and TNF and that are specific for Tag-peptide (Tag-T_H1 cells), induce IFN-γ- and TNFR1-dependent arrest of RIP1-Tag2 cancers (Supplementary Fig. 1a-c)[12]. This arrest occurs in the absence of significant T cell infiltration (Supplementary Fig. 1c, 2)[12] and is independent of either CTL[12] or enhanced apoptosis, as determined by TUNEL[12] or caspase-3 staining. Instead, Tag-specific T_H1 cells form follicle-like structures around the islets, where they interact with antigen-presenting cells[12]. Ki67 staining confirmed that Tag-T_H1 cells arrested

proliferation of β-cancers *in vivo* (Supplementary Fig. 3a). Freshly isolated β-cancer cells from Tag-T_H1 cell-treated RIP1-Tag2 mice failed to proliferate *in vitro* while β-cancer cells from sham-treated mice strongly incorporated ^{3}H-thymidine (Supplementary Fig. 3b). This suggests that T_H1 cytokines induce senescence *in vivo*, despite normal Tag-expression (Supplementary Fig. 4).

To directly ask whether IFN-γ and TNF induce senescence in β-cancers, we cultured freshly isolated β-cancer cells from sham-treated mice with either medium or with IFN-γ and TNF. In cell cycle analysis, untreated β-cancer cells were ≥25% in S phase and 40% in G_1/G_0, explaining their rapid proliferation. When combined, IFN-γ and TNF arrested most β-cancer cells in G_1/G_0 within three days (Fig. 1a). They reduced S phase cells to 3% and increased the G_1/S ratio 20-fold (Fig. 1b) without increasing the apoptotic sub-G_1 fraction (Fig. 1a). As IFN-γ and TNF arrested the β-cancer cells in G_1/G_0, a state characterizing cellular senescence, we asked whether IFN-γ and TNF caused senescence-defining permanent growth arrest.

Freshly isolated β-cancer cells proliferated rapidly in medium. When cultured in the presence of IFN-γ and TNF, β-cancer cells were fully growth arrested (Fig. 1c). To determine whether the growth-arrested β-cancer cells were really senescent, we washed the cells on day five and cultured them for another two weeks with medium only. While untreated β-cancer cells continued to expand, β-cancer cells that had been exposed for five days to the combination of IFN-γ and TNF were truly senescent as they remained fully growth-arrested (Fig. 1c). Even two weeks after withdrawal of IFN-γ and TNF, the β-cancer cells failed to incorporate BrdU while untreated controls strongly incorporated BrdU (Fig. 1d, e, Supplementary Fig. 5a, b).

IFN-γ and TNF also induced the characteristic senescence-associated

epigenetic and lysosomal changes, like nuclear recruitment of phosphorylated heterochromatin protein 1γ (pHP1γ) into senescence-associated heterochromatin foci (SAHF) or senescence-associated β-galactosidase (SA-β-gal) activity. Time course studies revealed that within three days, IFN-γ and TNF induced the early senescence marker pHP1γ in 75% (Supplementary Fig. 6a, b) and SA-β-gal in 50% of the β-cancer cells (Fig. 2a, b). Yet, induction of stable growth arrest and the late senescence marker SA-β-gal in 80% of the cells (Fig. 2c) needed ≥4 days of incubation with both IFN-γ and TNF. Double-staining with synaptophysin, an islet cell marker, confirmed SA-β-gal-expression by β-cancer cells (Supplementary Fig. 7). Combined IFN-γ and TNF established the senescence-defining permanent growth arrest in β-cancers cells while neither IFN-γ nor TNF alone was sufficient to induce full growth arrest (Supplementary Fig. 5a, b), although inducing early signs of senescence such as pHP1γ recruitment to SAFH (Supplementary Figure 6a, b), and SA-β-gal in 20% of the cells (Fig. 2b).

As combined stimulation of islets or islet tumors with IFN-γ and TNF strongly induces JunB[28], the combined IFN-γ/STAT1- and TNFR1-signaling may activate the JunB downstream target $p16^{Ink4a}$ and thus stabilize the $p16^{Ink4a}$/Rb senescence pathway in Tag-expressing β-cancers. Indeed, IFN-γ and TNF strongly induced $p16^{Ink4a}$ in subconfluent cultures within 48 hours (Fig. 2d), while $p16^{Ink4a}$ remained weakly expressed in medium-treated, subconfluent β-cancer cells (Fig. 2d). As this induction of $p16^{Ink4a}$ also caused sustained and severe hypophosphorylation of Rb at Ser795 (Fig. 2e) and suppressed the Rb-regulated gene E2F2[15] down to 20%, IFN-γ and TNF conjointly stabilized the $p16^{Ink4a}$/Rb senescence pathway in β-cancer cells. In line with this, STAT1- or TNFR1-deficient β-cancer cells fully resisted senescence

induction by IFN-γ and TNF, underlining that hypophosphorylation of Rb strictly required the combined action of the STAT1- and TNFR1-signaling pathways (Fig. 2b, f). As IFN-γ and TNF also induced senescence in unrelated breast cancers from polyoma virus middle T antigen (PyVmT)-transgenic mice (Supplementary Fig. 8) or human A204 rhabdomyosarcoma cells (Supplementary Fig. 9), cytokine-induced senescence was not restricted to Tag-expressing cancers.

Combined IFN-γ- and TNFR1-signaling is also necessary to arrest β-cancers *in vivo*[12] (Supplementary Fig. 1). Together the *in vitro* and *in vivo* data thus suggest that T_H1-immunity arrested cancer progression through IFN-γ- and TNF-induced senescence *in vivo*. To test this hypothesis, we first quantified senescence-associated chromatin changes by counting cancer cells positive for pHP1γ, trimethylated lysine-9 of histone 3 (H3K9me3), or apoptosis-associated active caspase-3 by immunohistology in either sham-treated mice or mice treated with Tag-T_H1 cells. T_H1-immunity significantly increased pHP1γ– and H3K9me3-positive nuclei in β-cancers, but not caspase-3-positive cells (Fig. 3a, b).

To address whether T_H1-immunity activated the $p16^{Ink4a}$/Rb pathway also *in vivo*, we double-stained sections for $p16^{Ink4a}$ and the proliferation marker Ki67. In sham-treated mice, the β-cancer cells were ≥30% Ki67-positive and only 5% $p16^{Ink4a}$-positive. T_H1-immunity diminished $Ki67^+$ cells to 3%, and increased the fraction of $p16^{Ink4a}$-positive cells (nuclear and cytoplasmic) to ≥20% (Figure 3c, d, Supplementary Fig. 10).

Senescence-induction by T_H1-immunity strictly required TNFR1-signaling also *in vivo*. $TNFR1^{-/-}$ β-cancers failed to increase either pHP1γ, H3K9me3, or active caspase-3 when treated with Tag-T_H1 cells (Supplementary Fig. 11a, b). In addition, whether isolated from sham- or Tag-T_H1 cell-treated mice, TNFR1-deficient β-cancer

cells expressed Ki67 but not $p16^{Ink4a}$ (Fig. 3c, d), even though Tag-T_H1 cells migrate into pancreata of TNFR1$^{-/-}$xRIP1-Tag2 mice[12]. As T_H1-immunity severely impaired β-cancer growth *in vivo*[12], these data strongly suggest that the combined IFN-γ- and TNFR1-signaling drove cancers into senescence also *in vivo*. Yet, the most stringent criterion defining senescence is stable and permanent growth arrest in the absence of T_H1-immunity[9,15-17].

We therefore cultured freshly isolated β-cancer cells from 12-week-old mice with medium only. Cells from sham-treated RIP1-Tag2 mice first suffered a critical loss and then re-initiated proliferation, yielding 10-20x10^5 β-cancer cells/pancreas after three passages (Fig. 4a). In contrast, β-cancer cells from RIP1-Tag2 mice treated with Tag-T_H1 cells were truly senescent, as they failed to proliferate over three passages and stably yielded only 0.5-2.0x10^5 cells/pancreas (Fig. 4a). β-cancer cells from TNFR1$^{-/-}$xRIP1-Tag2 mice grew exponentially also *in vitro*, yielding 100x10^5 cells within three passages, even when derived from Tag-T_H1 cell-treated mice (Fig. 4a).

To determine whether senescence was also maintained *in vivo*, we re-implanted the four different β-cancer cell lines after the 3rd passage under the skin of NOD-SCIDxIL2Rcγ$^{-/-}$ mice, as growth at ectopic sites characterizes cancers[2]. Within seven weeks, as few as 1.2x10^5 β-cancer cells from sham-treated RIP1-Tag2 mice significantly decreased blood glucose (Fig. 4b) and increased the serum insulin levels (Fig. 4c), demonstrating the metastatic potential of β-cancer cells from sham-treated mice. Senescent β-cancers from RIP1-Tag2 mice treated with Tag-T_H1 cells remained growth-arrested also *in vivo*, as blood glucose remained stable in all transplanted mice throughout the seven weeks (Fig. 4b). Minute adenomas in some NOD-SCIDxIL2Rcγ$^{-/-}$ mice and marginally increased serum insulin (Fig. 4c) showed

that the transplanted cells survived but remained growth-arrested for ≥10 weeks of *in vitro* and *in vivo* culture. Again, senescence-resistant TNFR1$^{-/-}$xRIP1-Tag2 β-cancer cells grew rapidly after transplantation and as little as 1.2x10^5 TNFR1$^{-/-}$ xRIP1-Tag2 cancer cells rapidly decreased blood glucose (Fig. 4b), irrespective of whether they were derived from sham-treated or Tag-T_H1 cell-treated mice. Transplanting 60% of total β-cancer cells from sham-treated RIP1-Tag2 mice generated tumors within seven weeks, while β-cancer cells from Tag-T_H1 cell-treated mice failed to grow (Fig. 4d). Only 10% of β-cancer cells from sham- or Tag-T_H1 cell-treated TNFR1$^{-/-}$xRIP1-Tag2 mice generated large tumors within the same time (Fig. 4d).

Oncogenes, DNA-damage or chemotherapeutics induce senescence that, in human cells, is reinforced by the senescence-associated secretome[14-17,29,30]. Uncovering that adaptive T_H1-immunity directly restrains cancer proliferation through IFN-γ/TNF-induced cancer cell senescence provides a long-searched direct mechanism explaining the anti-proliferative effects of T_H1-immunity on cancers[2,3]. T_H1-immunity has thus two majors effects on cancer, it can directly drive cancers into senescence and, subsequently, clear senescent cancer cells[9-11]. As these combined effects explain the therapeutic efficiency of tumor-specific T_H1-immunity in early cervical cancer[21] and disseminated melanoma[20], T_H1 cytokine-induced senescence may be of broad relevance for cancer control, also in humans under therapeutic conditions.

METHODS SUMMARY

RIP1-Tag2 and TNFR1$^{-/-}$xRIP1-Tag2 mice were either sham-treated or treated with Tag2-specific T_H1 cells starting at week 6. Cancer cells were isolated by consecutive collagenase/trypsin digestion from tumor tissues of RIP1-Tag2, STAT1$^{-/-}$xRIP1-Tag2, TNFR1$^{-/-}$xRIP1-Tag2, or PyVmT-transgenic mice. Isolated β-cancer cells were identified by immunofluorescence using anti-synaptophysin (early β-cell marker) antibodies. Proliferation *in vivo* and *in vitro* of tumor cells was measured by BrdU incorporation, Ki67 staining, ^{3}H-thymidine incorporation, or cell cycle analysis. Senescence was assessed by SA-β-gal staining, immunofluorescence, immunohistochemistry or Western blot using anti-pHP1-γ, anti–p16^{Ink4a}, anti-Rb, anti-phospho-Rb, or anti-H3K9me3 antibodies, or by *in vitro* and *in vivo* growth assays. Apoptosis was determined by cell cycle analysis, or immunohistochemistry with an anti-active caspase 3 antibody. For transfer experiments, β-cancer cells from sham- or T_H1 cell-treated mice (either RIP1-Tag2 or TNFR1$^{-/-}$x RIP1-Tag2) were injected subcutaneously into NOD-SCIDxIL2Rcγ$^{-/-}$ mice, and tumor growth was monitored with a caliper and by measuring blood glucose and insulin levels.

Full methods and any associated references are available in the online version of the paper at www.nature.com/nature.

1. Finn, O.J. Cancer immunology. *N. Engl. J. Med.* **358**, 2704-2715. (2008).
2. Hanahan, D. & Weinberg, R.A. Hallmarks of cancer: the next generation. *Cell* **144**, 646-674. (2011).
3. Schreiber, R.D., Old, L.J. & Smyth, M.J. Cancer immunoediting: integrating immunity's roles in cancer suppression and promotion. *Science* **331**, 1565-1570 (2011).
4. Koebel, C.M. et al. Adaptive immunity maintains occult cancer in an equilibrium state. *Nature* **450**, 903-907. (2007).
5. van den Broek, M.E. et al. Decreased tumor surveillance in perforin-deficient mice. *J. Exp. Med.* **184**, 1781-1790. (1996).
6. Willimsky, G. & Blankenstein, T. Sporadic immunogenic tumours avoid destruction by inducing T-cell tolerance. *Nature* **437**, 141-146. (2005).
7. Mocikat, R. et al. Natural killer cells activated by MHC class I(low) targets prime dendritic cells to induce protective CD8 T cell responses. *Immunity* **19**, 561-569. (2003).
8. Hung, K. et al. The central role of CD4(+) T cells in the antitumor immune response. *J Exp Med.* **188**, 2357-2368. (1998).
9. Xue, W. et al. Senescence and tumour clearance is triggered by p53 restoration in murine liver carcinomas. *Nature* **445**, 656-660. (2007).
10. Rakhra, K. et al. CD4(+) T cells contribute to the remodeling of the microenvironment required for sustained tumor regression upon oncogene inactivation. *Cancer Cell* **18**, 485-498. (2010).
11. Kang, T.W. et al. Senescence surveillance of pre-malignant hepatocytes limits liver cancer development. *Nature* **479**, 547-551 (2011).
12. Muller-Hermelink, N. et al. TNFR1 signaling and IFN-gamma signaling determine whether T cells induce tumor dormancy or promote multistage carcinogenesis. *Cancer Cell* **13**, 507-518. (2008).
13. Rocken, M. Early tumor dissemination, but late metastasis: insights into tumor dormancy. *J. Clin. Invest.* **120**, 1800-1803 (2010).
14. Braig, M. et al. Oncogene-induced senescence as an initial barrier in lymphoma development. *Nature.* **436**, 660-665. (2005).
15. Campisi, J. & d'Adda di Fagagna, F. Cellular senescence: when bad things happen to good cells. *Nat. Rev. Mol. Cell. Biol.* **8**, 729-740. (2007).
16. Collado, M. & Serrano, M. Senescence in tumours: evidence from mice and humans. *Nat Rev Cancer.* **10**, 51-57. (2010).
17. Nardella, C., Clohessy, J.G., Alimonti, A. & Pandolfi, P.P. Pro-senescence therapy for cancer treatment. *Nat. Rev. Cancer* **11**, 503-511 (2011).
18. Bergers, G., Javaherian, K., Lo, K.M., Folkman, J. & Hanahan, D. Effects of angiogenesis inhibitors on multistage carcinogenesis in mice. *Science* **284**, 808-812. (1999).
19. Casanovas, O., Hager, J.H., Chun, M.G. & Hanahan, D. Incomplete inhibition of the Rb tumor suppressor pathway in the context of inactivated p53 is sufficient for pancreatic islet tumorigenesis. *Oncogene* **24**, 6597-6604. (2005).
20. Hunder, N.N. et al. Treatment of metastatic melanoma with autologous CD4+ T cells against NY-ESO-1. *N. Engl. J. Med.* **358**, 2698-2703. (2008).
21. Kenter, G.G. et al. Vaccination against HPV-16 oncoproteins for vulvar intraepithelial neoplasia. *N. Engl. J. Med.* **361**, 1838-1847. (2009).
22. Hodi, F.S. et al. Improved survival with ipilimumab in patients with metastatic melanoma. *N. Engl. J. Med.* **363**, 711-723. (2010).

23. Schwartzentruber, D.J. et al. gp100 peptide vaccine and interleukin-2 in patients with advanced melanoma. *N. Engl. J. Med.* **364**, 2119-2127. (2011).
24. Morgan, R.A. et al. Cancer regression in patients after transfer of genetically engineered lymphocytes. *Science* **314**, 126-129. (2006).
25. Canova, C. et al. Genetic associations of 115 polymorphisms with cancers of the upper aerodigestive tract across 10 European countries: the ARCAGE project. *Cancer Res.* **69**, 2956-2965. (2009).
26. Critchley-Thorne, R.J. et al. Impaired interferon signaling is a common immune defect in human cancer. *Proc. Natl. Acad. Sci. U. S. A.* **106**, 9010-9015. (2009).
27. Zhang, B., Karrison, T., Rowley, D.A. & Schreiber, H. IFN-gamma- and TNF-dependent bystander eradication of antigen-loss variants in established mouse cancers. *J. Clin. Invest.* **118**, 1398-1404. (2008).
28. Gurzov, E.N. et al. Pancreatic beta-cells activate a JunB/ATF3-dependent survival pathway during inflammation. *Oncogene.* **31**, 1723-1732. doi: 1710.1038/onc.2011.1353. Epub 2011 Aug 1715. (2012).
29. Kuilman, T. et al. Oncogene-induced senescence relayed by an interleukin-dependent inflammatory network. *Cell* **133**, 1019-1031. (2008).
30. Acosta, J.C. et al. Chemokine signaling via the CXCR2 receptor reinforces senescence. *Cell* **133**, 1006-1018. (2008).

Supplementary Information is linked to the online version of the paper at www.nature.com/nature

Acknowledgements The authors thank A. Knuth, H.G. Rammensee, K. Ghoreschi, L. Zender and G. Riethmüller for helpful discussions. The excellent technical assistance of S. Weidemann and M. Dierstein is gratefully acknowledged. This work was supported by the Sander Stiftung (2005.043.2 and 2005.043.3), the Deutsche Krebshilfe (No. 109037), the IZKF-Promotionskolleg „Molekulare Medizin“ 2010 (1886-0-0), the Deutsche Forschungsgemeinschaft (SFB 685, SFB 773 and Wi 1279/3-1) and in part by the German Federal Ministry of Education and Research (BMBF) to the German Center for Diabetes Research (DzD e.V.).

Author Contributions H.B., T.W., R.M., K.S.-O. and M.R. developed the concept based on original data and concepts of M.R., and designed the experiments. H.B., T.W., S.F., M.K., C.G., F.E., M.H., K.B., T.M. and E.B. performed experiments and analysed the data. B.F. and M.S. established and carried out fluorescence microscopy. L.Q.-M.d.F. and F.F. performed light microscopy and advised on cell biology. M.A., K.S. and R.H. superwised and performed the β-cancer cell transfer experiments. F.R., S.U. and H.-U.H. isolated β-cancer cells and advised on β-cell physiology. H.B., T.W., M.v.d.B., K.S.-O. and M.R. interpreted the data and wrote the paper.

Author Information Reprints and permissions information is available at www.nature.com/reprints. The authors declare no competing financial interests. readers are welcome to comment on the online version of this article at www.nature.com/nature Correspondence and requests for materials should be addressed to M.R. (mrocken@med.uni-tuebingen.de).

Figure Legends

Fig. 1 | Combined, the T_H1 cytokines IFN-γ and TNF induce stable growth arrest of Tag-driven β-cancer cells *in vitro*.
a, b, Cell cycle analysis (**a**) and mean G1/S ratio (**b**) of β-cancer cells cultured either in the absence or presence of IFN-γ and TNF. **c-e,** Cell numbers (**c**), BrdU incorporation (**d**) and mean numbers of BrdU-positive spots (**e**) of β-cancer cells treated for five days with medium only or with IFN-γ and TNF. Thereafter, cells were washed and then cultured with medium in the absence of cytokines for another two passages. After the second passage 3,000 viable cells were seeded in 96 well plates and cell proliferation was analyzed by BrdU staining.
P*<0.05. n=3-6 (b, c, e**). Control=Co. (**a-e**).

Fig. 2 | STAT1- and TNFR1-dependent stabilization of the $p16^{Ink4a}$/Rb senescence pathway in β-cancer cells by the combined action of IFN-γ and TNF *in vitro*.
a, SA-β-gal activity of β-cancer cells after 72 h of treatment with medium, IFN-γ, TNF, or IFN-γ and TNF. Bar, 100 µm. **b,** Concentration-dependent induction of SA-β-gal^+ cells by TNF either in the absence or presence of IFN-γ within 72 h in β-cancer cells from RIP1-Tag2 or $TNFR1^{-/-}$xRIP1-Tag2 mice. **c,** Induction of SA-β-gal activity by IFN-γ and TNF within 96 h. **d,** Detection of $p16^{Ink4a}$ or β-actin by Western blot in β-cancer cells treated with medium or with IFN-γ and TNF. **e,** Detection of phosphorylated Rb (p-Rb), total Rb (Rb), or β-actin by Western blot in β-cancer cells treated with medium or IFN-γ and TNF. **f,** SA-β-gal activity of β-cancer cells isolated from either RIP1-Tag2 or $STAT1^{-/-}$xRIP1-Tag2 mice after 72 h of treatment with medium or with IFN-γ and TNF.
P*<0.05. n=3-9 (b,c,f**). Control=Co. (**a, c-f**).

Fig. 3 | TNFR1-dependent induction of growth arrest and senescence in β-cancer cells by T_H1-immunity *in vivo*.
a, b, Analysis of the senescence markers pHP1γ and tri-methylated H3K9 (H3K9me3), or the apoptosis marker active caspase-3 by immunohistochemistry (**a**), and percentage (**b**) of pHP1γ-, H3K9me3- or active caspase-3-positive cells in β-cancers from RIP1-Tag2 mice that were either sham- or Tag-T_H1 cell-treated. Bar, 100 µm. **c, d,** Double-staining (**c**) for the senescence marker $p16^{Ink4a}$ (red) and the proliferation marker Ki67 (blue), and percentage (**d**) of $p16^{Ink4a}$- and Ki67-positive cells in cancers from RIP1-Tag2 or $TNFR1^{-/-}$xRIP1-Tag2 mice that were sham- or Tag-T_H1 cell-treated. Nuclei are green. Bar, 25 µm.
P*<0.05 from sham-treated control. n=5-6 (b, d**).

Fig. 4 | T_H1-immunity induces TNFR1-dependent, permanent growth arrest of β-cancer cells which remains stable for ≥10 weeks, even after transfer into immune-deficient NOD-SCIDxIL2Rc$\gamma^{-/-}$ mice.
a, Cell numbers of β-cancer cells isolated from RIP1-Tag2 or $TNFR1^{-/-}$xRIP1-Tag2 mice that were sham- or Tag-T_H1 cell-treated. The number of cell passages (p) is indicated, and the data are presented as number of living β-cancer cells per mouse.

b, Blood glucose levels in NOD-SCIDxIL2Rc$\gamma^{-/-}$ mice after transfer of $1.2x10^5$ β-cancer cells isolated from sham- or Tag-T_H1 cell-treated RIP1-Tag2 or TNFR1$^{-/-}$ xRIP1-Tag2 mice. **c,** Insulin levels in NOD-SCIDxIL2Rc$\gamma^{-/-}$ mice after transfer of $1.2x10^5$ β-cancer cells isolated from sham- or Tag-T_H1 cell-treated RIP1-Tag2 mice. **d,** Tumor volumes in NOD-SCIDxIL2Rc$\gamma^{-/-}$ mice after transfer of β-cancer cells isolated from sham- or Tag-T_H1 cell-treated mice. The table indicates origin and percentage of total β-cancer cells/mouse injected.
Red lines: blood glucose of untreated NOD-SCIDxIL2Rc$\gamma^{-/-}$ mice (**b**). Dashed red lines: normal range of insulin in healthy mice (**c**).
*P<0.05 from sham-treated control. n=3-6 (**a-d**).

METHODS

Animals. C3H mice from Charles River (Sulzberg, Germany), transgenic RIP1-Tag2 mice[31], double transgenic TNFR1$^{-/-}$xRIP1-Tag2[12, 32] and STAT1$^{-/-}$xRIP1Tag2 mice (backcross of STAT$^{-/-}$ mice from Taconic (Hudson, NY, USA) over 12 generations to C3H), TCR2 mice[33] all on a C3H background, and PyVmT-transgenic mice[34] were bred under specific pathogen-free conditions. NOD-SCIDxIL2Rc$\gamma^{-/-}$ mice (NOD.Cg-Prkdc^{scid} IL2rcγ^{tm1Wjl}/SzJ)[35] were from The Jackson Laboratory (Bar Harbor, ME, USA). Animal experiments were approved by the local authorities (HT 2/03, HT2/07 and K1/07).

Cell culture and single cell analysis. Tag-specific T_H1 cells were isolated and generated from TCR2 mice, and characterized by flow cytometry[12].

Tumors were isolated from sham- and Tag-T_H1-cell-treated RIP1-Tag2 mice, sham- and Tag-T_H1-cell-treated TNFR1$^{-/-}$xRIP1-Tag2 mice, STAT1$^{-/-}$xRIP1-Tag2 mice, or mammary tumor-bearing PyVmT-transgenic mice by collagenase digestion (1 mg/ml, Serva, Heidelberg, Germany) for 10 min at 37°C, and then separated under a dissection microscope (Leica Microsystems, Wetzlar, Germany). Tumor cells were obtained by incubation in 0.05% trypsin/EDTA solution (Invitrogen, Darmstadt, Germany) at 37°C for 10 min, and seeded on tissue culture plates. Adherent cells were cultured for 2 to 5 weeks in RPMI 1640 supplemented with 10% fetal calf serum, nonessential amino acids, antibiotics, and 50 µM 2-mercaptoethanol at 37°C and 5% CO_2. Human rhabdomyosarcoma cells (A204 cells) were grown in complete RPMI 1640 medium. If not otherwise stated, subconfluent cells were treated with 100 ng/ml mouse or human IFN-γ (R&D Systems, Wiesbaden, Germany), or 10 ng/ml mouse or human TNF (R&D Systems), or with a combination of mouse or human IFN-γ (50-100 ng/ml) and mouse or human TNF (0.1-10 ng/ml) for 2-6 d. β-cancer

cells were identified by immunofluorescence using an anti-synaptophysin antibody (undiluted; Lifespan Biosciences, Seattle, WA, USA).

***In vitro* proliferation assays.** After treatment, cancer cell proliferation was measured either by the [^{3}H]-thymidine incorporation assay[36], or by the BrdU-based Cell Proliferation ELISA and XTT-based Cell Proliferation Kit II according to the manufacturer´s protocols (Roche Diagnostics, Mannheim, Germany). [^{3}H]-thymidine incorporation was quantified using a MicroBeta TriLux counter (PerkinElmer, Rodgau, Germany), and colorimetric analyses were performed on a Multiskan EX microplate reader (Thermo Electron, Erlangen, Germany).

***In vitro* growth arrest assays.** The different cancer cells were seeded at a density of 1 x 10^4 cells/cm^2. Then, the cells were treated with control medium or cytokines as described above for 4-5 d. After treatment, the cells were trypsinized and viable cells (trypan blue exclusion) were counted under a Zeiss Axiovert 25 microscope (Zeiss, Oberkochen, Germany) using a Neubauer counting-chamber (Karl Hecht GmbH, Sondheim, Germany). The cells were seeded at 2 x 10^4 cells/cm^2 and grown in complete RPMI 1640 medium until the control cultures reached confluence. Then, the cells were trypsinized, counted and seeded again. After passage 1-2 (p1-p2), 1000-3000 viable cells were seeded on Multiscreen^{TM} HTS 96 well Filtration Plates (Millipore, Billerica, MA, USA), and proliferation was measured by the BrdU-based Cell Proliferation ELISA (Roche Diagnostics) in combination with the Vector$^{®}$SG Substrate Kit for Peroxidase from Vector Laboratories (Burlingame, CA, USA) to visualize BrdU-incorporating cells. BrdU-positive spots were counted with an ELISPOT reader (Bioreader$^{®}$-3000; BIO-SYS, Karben, Germany). In addition, some cultures were stained with DAPI (Invitrogen) to visualize the nuclei of adherent cells.

Treatment of mice with Tag-T_H1 cells. Before the first Tag-T_H1-cell-based therapy, all mice received 2 Gy total-body irradiation. Then, 1 x 10^7 Tag-T_H1 cells in 0.9% NaCl solution (Tag-T_H1) or NaCl solution alone (Sham) was injected intraperitoneally once per week starting at week 6^{12}. If not otherwise stated, mice were sacrificed at week 12.

Transfer of β-cancer cells into immune-deficient mice. β-cancer cells isolated from the various groups of mice were cultured for 3 passages. Then, 10-60% of the β-cancer cells were injected subcutaneously (s.c.) into immune-deficient NOD-SCIDxIL2Rc$\gamma^{-/-}$ mice. Tumor growth was monitored with a caliper, and blood glucose was measured using an Accu-Check sensor (Roche Diagnostics) for up to 7 weeks. Serum insulin levels were determined using the rat/mouse insulin ELISA kit from Millipore.

Immunofluorescence and immunohistochemistry. The different cancer cells were grown on chamber slides (BD Biosciences, Heidelberg, Germany). After treatment, the cells were fixed with acetone/methanol 1:1. The slides were washed with PBS/0.05% Tween 20 at room temperature (RT), blocked with serum-free DAKO-Block (DAKO, Hamburg, Germany), washed again, and then incubated with the following antibodies: anti-Ki67 (dilution 1:100; Abcam, Cambridge, UK), anti-PCNA (dilution 1:100; Cell Signaling Technology, Boston, MA, USA), anti-pHP1γ (dilution 1:100; Abcam), anti-H3K9me3 (dilution 1:500; Millipore, Schwalbach, Germany), anti-$p16^{Ink4a}$ (dilution 1:100; Santa Cruz Biotechnology, Heidelberg, Germany), anti-SV40 Large T Antigen (dilution 1:100; BD Biosciences), or anti-synaptophysin (undiluted; Lifespan Biosciences). After washing, the slides were incubated with anti-rabbit Alexa488 (Invitrogen), anti-rabbit-Cy3 (Dianova, Hamburg, Germany), anti-mouse Alexa555, or anti-mouse Alexa488 (both from Cell Signaling Technology), washed

again and incubated with DAPI (Invitrogen). Finally, the slides were washed, mounted with fluorescence mounting medium (DAKO) and analyzed using a Zeiss Axiovert 200 microscope (Zeiss) with the Visiview software (Visitron Systems, Puchheim, Germany).

Fresh frozen cryostat sections of whole pancreata were stained as described[36]. Briefly, the sections were fixed with periodate-lysine-paraformaldehyde, blocked with donkey serum (dilution 1:20), and then incubated with rabbit anti-pHP1γ (dilution 1:80), mouse anti-PCNA (dilution 1:50), mouse anti-$p16^{Ink4a}$ (dilution 1:50), or rabbit anti-Ki67 antibodies (dilution 1:100). After washing, the sections were incubated with Cy3-conjugated donkey anti-rabbit, donkey anti-mouse, or Cy5-conjugated donkey-anti-rabbit, donkey-anti-mouse IgG (all from Dianova). Before mounting the slides with Mowiol (Hoechst, Frankfurt, Germany), nuclei were stained with Yopro (1:2000; Invitrogen). The sections were analyzed using a Leica TCS-Sp/Leica DM RB confocal laser scanning microscope (Leica Microsystems). Images were processed with the Leica Confocal Software LCS (Version 2.61).

Formalin-fixed pancreata were embedded in paraffin. Sections (3-5 µm thick) were cut and stained with H&E. Immunohistochemistry was performed on an automated immunostainer (Ventana Medical System, Tucson, AZ, USA), according to the manufacturer's protocol, with minor modifications[37]. The antibody panel used included activated caspase-3 (Cell Signaling Technology), Ki-67 (DCS Innovative Diagnostic Systeme, Hamburg, Germany), pHP1-γ (Abcam), and H3K9me3 (Cell Signaling Technology).

SA-β-galactosidase activity assay. Cancer cells were fixed for 15 min at RT, and then stained for 16 h at 37°C using the β-Galactosidase Staining Kit (United States Biological; Swampscott, MA, USA). SA-β-gal-positive and -negative cells were then

counted using a Zeiss Axiovert 200 microscope (Zeiss). In some experiments, the cells were counterstained for synaptophysin by immunofluorescence, and synaptophysin/SA-β-gal double-positive cells were counted.

Cell cycle analysis. After treatment of β-cancer cells, cell cycle analysis was performed using the BD Pharmingen™ FITC-BrdU Flow Kit according to the manufacturer´s protocol (BD Biosciences). The samples were analyzed by flow cytometry on a LSR II from Becton Dickinson (Heidelberg, Germany), and the following cell cycle phases were determined in % of the total population: $subG_1$ (apoptotic cells), G_1/G_0 (2n, BrdU-negative), S (2n-4n, BrdU-positive) and G_2/M phase (4n, BrdU-negative).

Western blot. After treatment, cancer cells were lysed in lysis buffer (50 mM Tris-HCl, pH 7.5, 150 mM NaCl, 1% Triton X-100, 0.5% SDS, 1mM NaF, 1mM Na_3VO_4, and 0.4% β-mercaptoethanol) containing a protease inhibitor cocktail and a phosphatase inhibitor cocktail (PhosSTOP from Roche Diagnostics). Alternatively, cytoplasmic protein extracts were obtained from the cell cultures using the NE-PER extraction kit (Thermo Fisher Scientific, Rockford, IL, USA) according to the manufacturer´s protocol. Before use, protease inhibitors and PhosSTOP were added to the lysis buffers CER I and NER. After determination of protein content by the bicinchoninic acid assay (BCA; Thermo Fisher Scientific), proteins were resolved by 12% SDS-PAGE or by Mini Protean TGX Precast Gels (4-15%; from BioRad, München, Germany), transferred onto a PVDF membrane and blocked with 3% nonfat milk in TBS/0.1% Tween 20 (TBST) as described[38]. The membrane was incubated with anti-$p16^{Ink4a}$ (1:1000; Santa Cruz), anti-Rb (Ab-780) (1:1000), anti-Rb(phospho-Ser-795) (1:1000; both from SAB Signalway Antibody, Pearland, TX, USA), or anti-β-actin antibody (1:1000; BioVision, Mountain View, CA, USA). After

washing with TBST and subsequent blocking, the blots were incubated with goat anti-mouse horseradish-peroxidase (HRP)-conjugated antibody or with goat anti-rabbit horseradish-peroxidase (HRP)-conjugated antibody (1:3000; Cell Signaling Technology), washed again and antibody binding was detected with the ECL detection reagent (Amersham, Freiburg, Germany). Immunoreactive bands were quantified using the ImageJ software (National Institute of Health, Bethesda, MD, USA), and the phospho-Rb/Rb ratio of the samples was calculated.

Statistics. Data are expressed as arithmetic means ± S.E.M. and statistical analyses were made by unpaired *t*-test, or ANOVA using Dunnett´s or Tukey´s test as post hoc test, where appropriate. $P<0.05$ was considered statistically different.

31. Hanahan, D. Heritable formation of pancreatic beta-cell tumours in transgenic mice expressing recombinant insulin/simian virus 40 oncogenes. *Nature* **315**, 115-122. (1985).
32. Pfeffer, K. et al. Mice deficient for the 55 kd tumor necrosis factor receptor are resistant to endotoxic shock, yet succumb to L. monocytogenes infection. *Cell* **73**, 457-467. (1993).
33. Forster, I., Hirose, R., Arbeit, J.M., Clausen, B.E. & Hanahan, D. Limited capacity for tolerization of CD4+ T cells specific for a pancreatic beta cell neo-antigen. *Immunity* **2**, 573-585. (1995).
34. Maglione, J.E. et al. Transgenic Polyoma middle-T mice model premalignant mammary disease. *Cancer Res.* **61**, 8298-8305. (2001).
35. Shultz, L.D., Ishikawa, F. & Greiner, D.L. Humanized mice in translational biomedical research. *Nat. Rev. Immunol.* **7**, 118-130. (2007).
36. Kneilling, M. et al. Direct crosstalk between mast cell-TNF and TNFR1-expressing endothelia mediates local tissue inflammation. *Blood* **114**, 1696-1706. (2009).
37. Kunder, S. et al. A comprehensive antibody panel for immunohistochemical analysis of formalin-fixed, paraffin-embedded hematopoietic neoplasms of mice: analysis of mouse specific and human antibodies cross-reactive with murine tissue. *Toxicol. Pathol.* **35**, 366-375. (2007).
38. Hennige, A.M. et al. Overexpression of kinase-negative protein kinase Cdelta in pancreatic beta-cells protects mice from diet-induced glucose intolerance and beta-cell dysfunction. *Diabetes* **59**, 119-127 (2009).

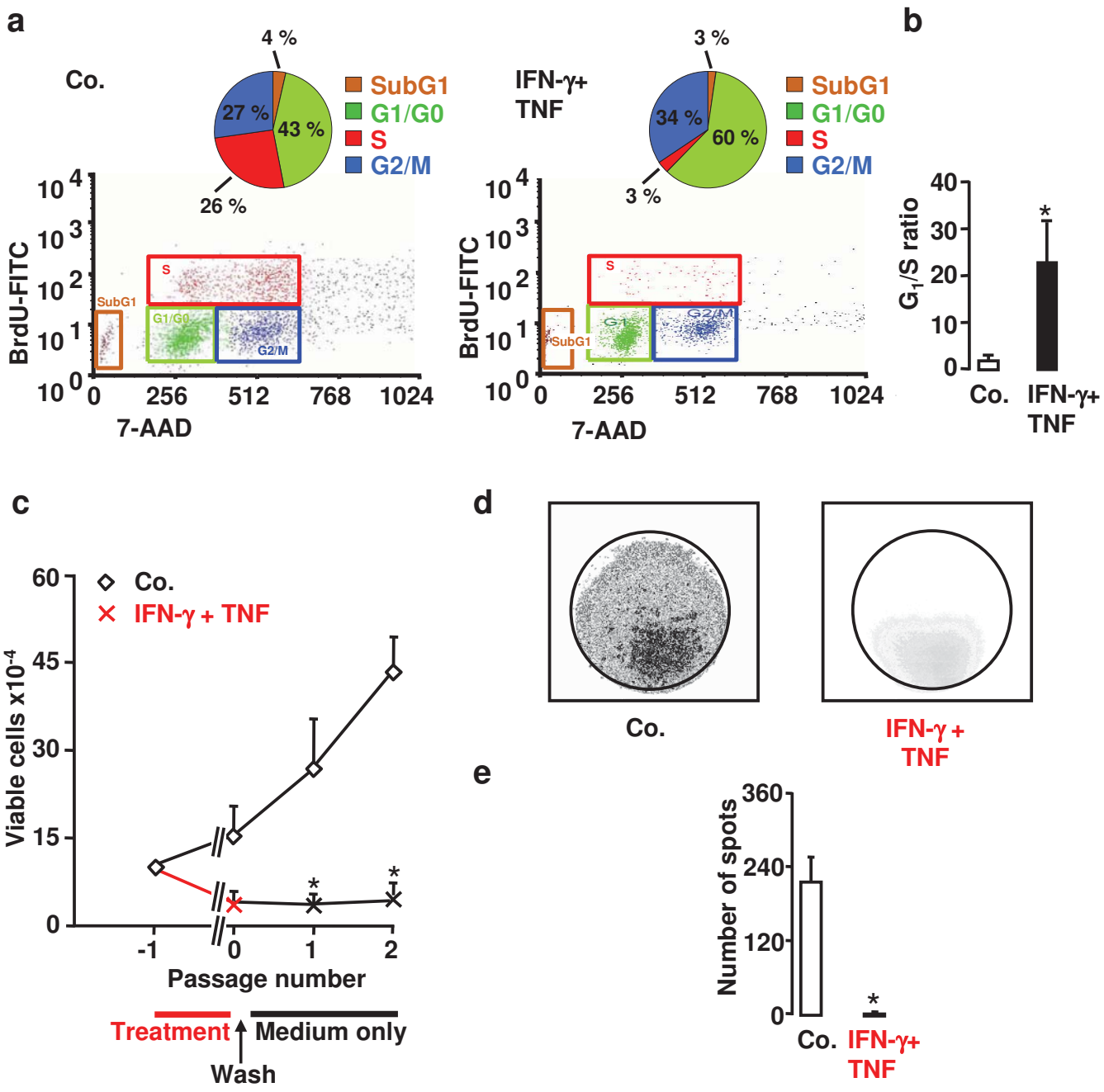
a
Co.
4 %
27 %
43 %
26 %
SubG1
G1/G0
S
G2/M
BrdU-FITC
7-AAD
IFN-γ+
TNF
3 %
34 %
60 %
3 %
b
G1/S ratio
Co.
IFN-γ+
TNF
c
Co.
IFN-γ + TNF
Viable cells x10-4
Passage number
Treatment
Medium only
Wash
d
Co.
IFN-γ +
TNF
e
Number of spots
Co.
IFN-γ+
TNF

Fig. 1

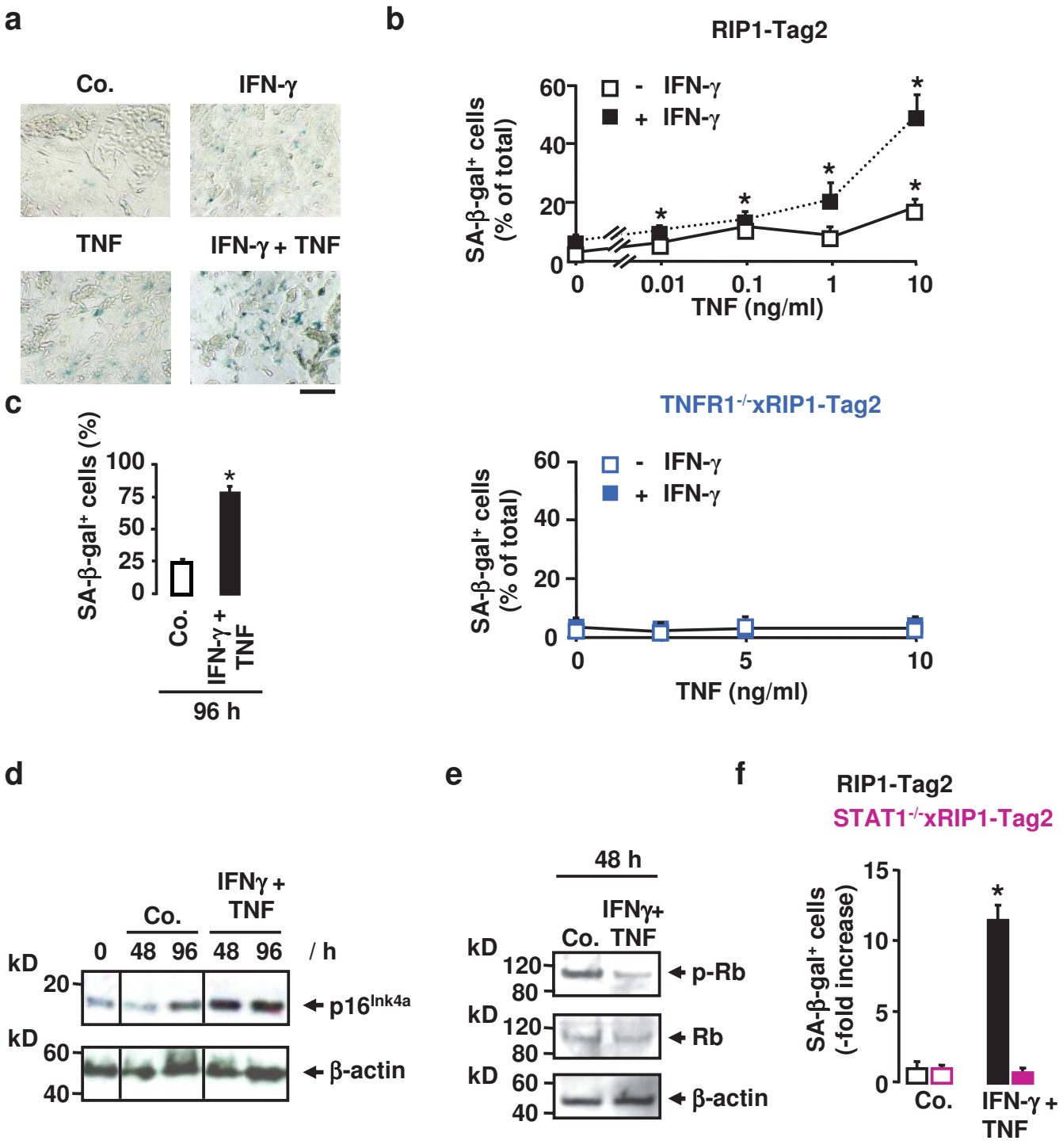
a
Co.
IFN-γ
TNF
IFN-γ + TNF
b
RIP1-Tag2
SA-β-gal+ cells (% of total)
- IFN-γ
+ IFN-γ
TNF (ng/ml)
TNFR1-/-xRIP1-Tag2
c
SA-β-gal+ cells (%)
Co.
IFN-γ + TNF
96 h
d
IFNγ + TNF
Co.
/ h
kD
p16Ink4a
β-actin
e
48 h
IFNγ+ TNF
p-Rb
Rb
β-actin
f
RIP1-Tag2
STAT1-/-xRIP1-Tag2
SA-β-gal+ cells (-fold increase)

Fig. 2

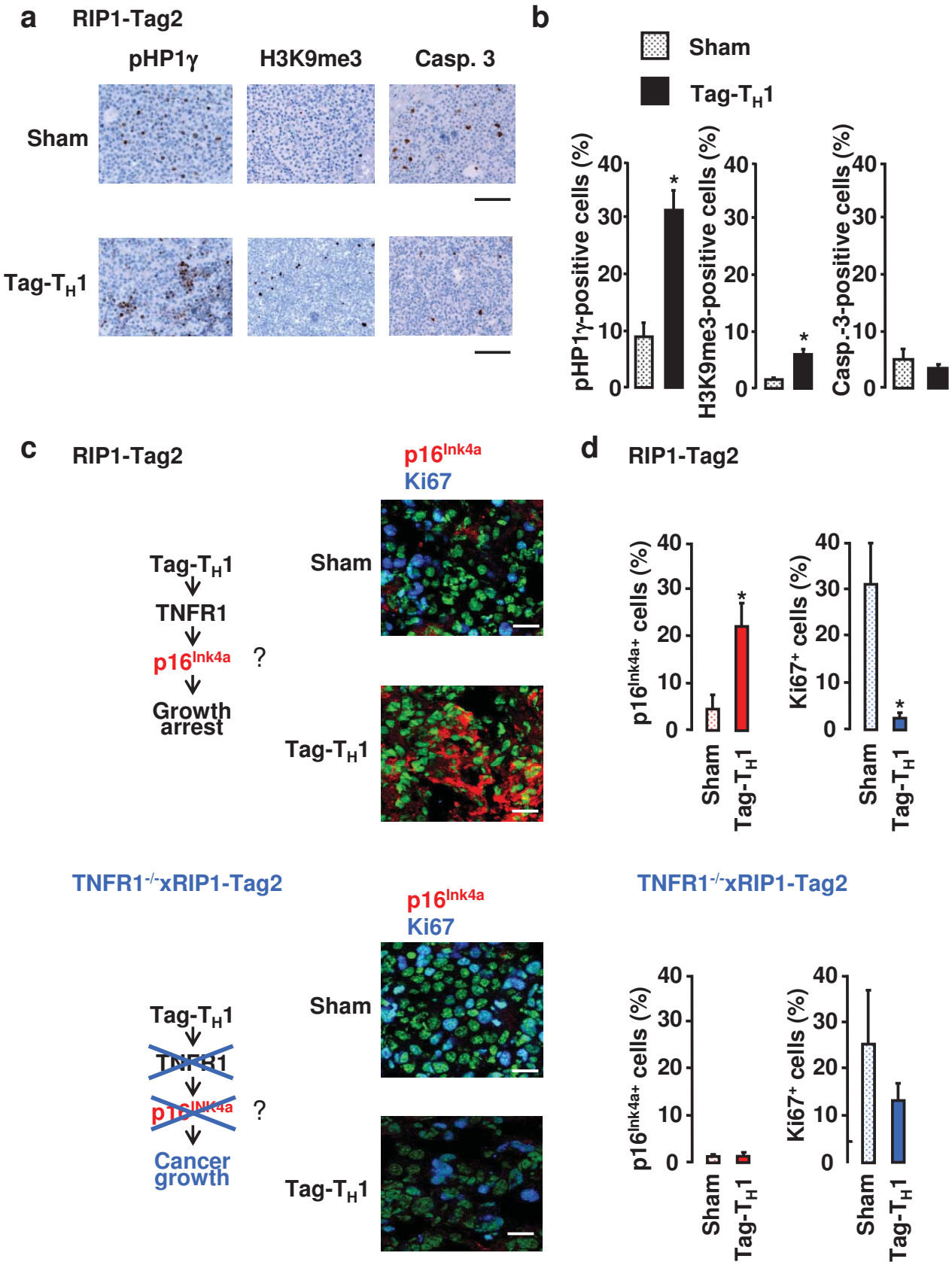
a
RIP1-Tag2
pHP1γ
H3K9me3
Casp. 3
Sham
Tag-TH1
b
Sham
Tag-TH1
pHP1γ-positive cells (%)
H3K9me3-positive cells (%)
Casp.-3-positive cells (%)
0
10
20
30
40
*
c
RIP1-Tag2
p16Ink4a
Ki67
Tag-TH1
TNFR1
p16Ink4a
?
Growth arrest
Sham
Tag-TH1
d
RIP1-Tag2
p16Ink4a+ cells (%)
Ki67+ cells (%)
Sham
Tag-TH1
TNFR1-/-xRIP1-Tag2
p16Ink4a
Ki67
Tag-TH1
TNFR1
p16Ink4a
?
Cancer growth
Sham
Tag-TH1
TNFR1-/-xRIP1-Tag2
p16Ink4a+ cells (%)
Ki67+ cells (%)
Sham
Tag-TH1

Fig. 3

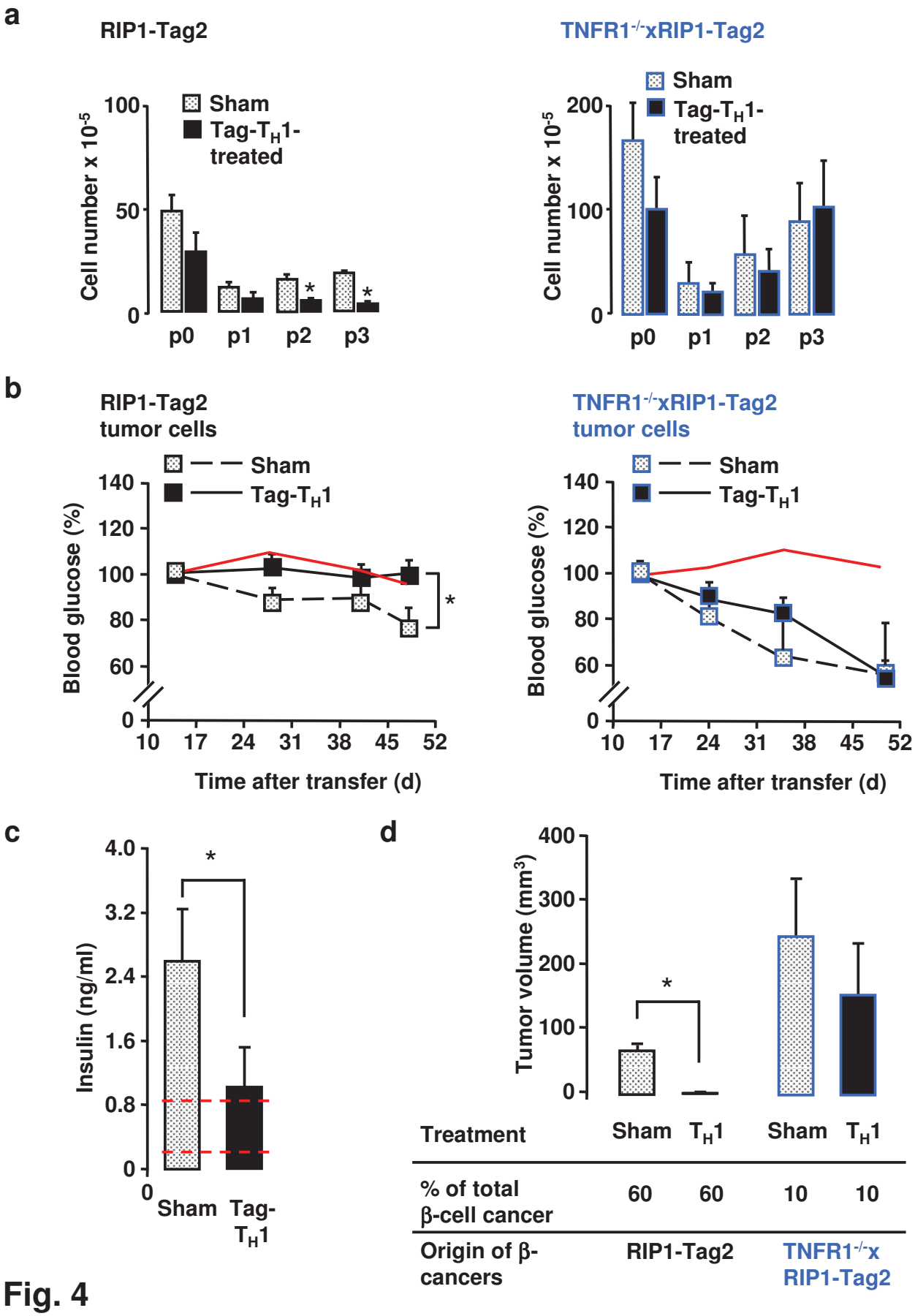
a
RIP1-Tag2
TNFR1-/-xRIP1-Tag2
Sham
Tag-TH1-treated
Cell number x 10-5
100
50
0
200
100
p0
p1
p2
p3
*
b
RIP1-Tag2 tumor cells
TNFR1-/-xRIP1-Tag2 tumor cells
Sham
Tag-TH1
Blood glucose (%)
140
120
100
80
60
10
17
24
31
38
45
52
Time after transfer (d)
c
Insulin (ng/ml)
4.0
3.2
2.4
1.6
0.8
Sham
Tag-TH1
d
Tumor volume (mm3)
400
300
200
Treatment
Sham
TH1
% of total β-cell cancer
60
10
Origin of β-cancers
RIP1-Tag2
TNFR1-/-x RIP1-Tag2

Fig. 4